Journal of Molecular Catalysis A: Chemical 407 (2015) 25–31

Contents lists available at ScienceDirect

Journal of Molecular Catalysis A: Chemical

journal homepage: www.elsevier.com/locate/molcata

Enhancement of visible light photocatalytic activity of Ag_2O/F-TiO_2 composites

Wei Yu[a], Xinjuan Liu[b,*], Haipeng Chu[b], Guang Zhu[c], Jinliang Li[a], Junying Liu[a], Lengyuan Niu[b], Zhuo Sun[a], Likun Pan[a,**]

[a] Engineering Research Center for Nanophotonics & Advanced Instrument, Ministry of Education, Department of Physics, East China Normal University, Shanghai 200062, China
[b] Institute of Coordination Bond Metrology and Engineering, College of Materials Science and Engineering, China Jiliang University, Hangzhou 310018, China
[c] Anhui Key Laboratory of Spin Electron and Nanomaterials, Suzhou University, Suzhou 234000, China

ARTICLE INFO

Article history:
Received 17 March 2015
Received in revised form 5 June 2015
Accepted 10 June 2015
Available online 16 June 2015

Keywords:
Ag_2O/F-TiO_2
Coprecipitation method
Photocatalytic
Methylene blue (MB)

ABSTRACT

We synthesized the Ag_2O/F-TiO_2 composites *via* an aqueous precipitation method and characterized their morphology, structure and photocatalytic activity in the degradation of methylene blue (MB) using scanning electron microscopy, transmission electron microscopy, X-ray diffraction, X-ray photoelectron spectroscopy, UV–vis absorption spectroscopy, and electrochemical impedance spectra, respectively. The results show that the Ag_2O addition could enhance the visible light photocatalytic activity of Ag_2O/F-TiO_2 composites with a maximum MB degradation rate of 93% for 60 min, much higher than that of the F-TiO_2 (30%). The excellent photocatalytic activity is due to the increased visible light absorption, and promoted separation of photo-generated electrons and holes in F-TiO_2 with the introduction of Ag_2O.

1. Introduction

Photocatalysis has already attracted significant interest worldwide, due to its potential applications in many areas including clean energy production [1–4], environment remediation and chemical reaction technologies [5–19]. Exploring visible light-responsive photocatalysts with good photocatalytic performance is one of the core issues for photocatalysis. Currently, doping with nonmetal elements such as N, C, F and B was demonstrated to be an effective approach to enhance the visible light photocatalytic activity of wide semiconductor [20,21]. In particular, F doped TiO_2 (F-TiO_2) has been proven to be a promising visible light photocatalyst [22–26]. The F doping in TiO_2 can increase the visible light absorption and reduce electron–hole pair recombination by creating of oxygen vacancies and Ti^{3+} surface states in TiO_2 [27,28], leading to the enhancement of photocatalytic activity of TiO_2. However, the quick recombination of photo-generated charge carriers still exists in F-TiO_2 and significantly decreases its photocatalytic activity.

Currently, a particularly attractive strategy is to design and develop hybrid materials based on F-TiO_2 to overcome the aforementioned problems. TiN/, Bi2O3/ and CuO/F-TiO_2 composites have been found to exhibit excellent visible light photocatalytic activity compared with F-TiO_2 [29–31]. Ag_2O with a narrow energy band gap of ~1.2 eV has been found to be an efficient visible light photocatalyst [32–35]. Ag_2O-based composites have been demonstrated with the excellent visible light photocatalytic activity owing to the synergistic effects on promoting the generation and separation of the photo-generated electron–hole pairs [34–38]. Therefore, development of composite material based on Ag_2O and F-TiO_2 should be a promising method to enhance the visible light photocatalytic activity of F-TiO_2 because of the stepwise structure of band-edge levels constructed in the Ag_2O/F-TiO_2 (AT) composites (Scheme 1). The conduction band (CB) of TiO_2 is −0.34 V and valence band (VB) 2.86 V (*vs.* SHE) [39,40], while the corresponding values of Ag_2O are 0.20 and 1.40 V (*vs.* SHE), respectively [35,36,41]. Such energy levels are beneficial to the transfer of photo-induced electrons from F-TiO_2 CB to Ag_2O CB, which could efficiently separate the photo-induced electrons and hinder the charge recombination in the electron-transfer processes, thus enhance the photocatalytic performance. Unfortunately, there has been no report on the synthesis and application of AT composites in photocatalysis to date.

In this work, AT composites were synthesized *via* an aqueous precipitation method. The as-synthesized AT composites exhibit an enhanced photocatalytic activity in the degradation of methylene blue (MB) under visible light irradiation compared with the F-TiO_2.

* Corresponding author. Fax: +86 57186872475.
** Corresponding author. Fax: +86 21 62234132.
E-mail addresses: lxj669635@126.com (X. Liu), lkpan@phy.ecnu.edu.cn (L. Pan).

http://dx.doi.org/10.1016/j.molcata.2015.06.015
1381-1169/

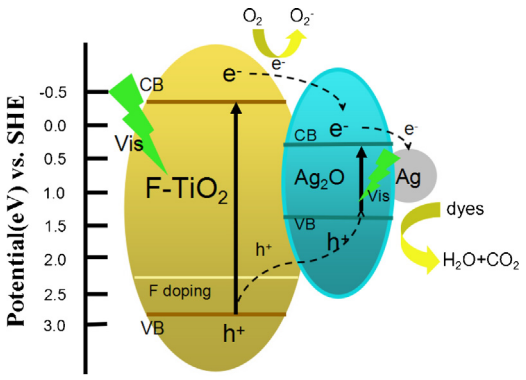

Scheme 1. Schematic diagram of energy levels of F-TiO_2 and Ag_2O.

The possible photocatalytic mechanism for the photo-degradation process over AT composites was also studied in terms of a series of characterization.

2. Experimental

2.1. Synthesis of F-TiO_2

F-TiO_2 was prepared by a sol–gel method [26]. 8 ml of tetrabutyl titanate was first dissolved in 15 ml of ethanol by stirring for 30 min at room temperature to obtain solution A. 390 mg NH4F was dissolved in 14 ml ethanol, and then 5 ml acetic acid and 2 ml deionized water were successively added into the solution with stirring for 30 min at room temperature to obtain solution B. Solution B was then added dropwise into solution A under vigorous stirring. Subsequently, the mixture solution was continuously stirred at room temperature for the hydrolysis of tetrabutyl titanate until a transparent sol was formed. Finally, the sol was dried in air at 100 °C for 24 h, ground and heated at 500 °C for 1 h.

2.2. Synthesis of Ag_2O/F-TiO_2 composite

A certain amount of $AgNO_3$ solution, 0.4 g F-TiO_2 powder and 2 g polyethylene glycol (average molecular weight 200) were dissolved in 100 ml water by sonication for 15 min to produce a uniform dispersion. Then a dilute NaOH solution was dropped in above solution to adjust the pH value to be 13, and the mixture was stirred for 30 min. The AT samples synthesized using 0.02, 0.03, 0.04 mol AgNO3, named as T1, T2 and T3, were isolated by filtration, washed three times with distilled water, and finally dried at 80 °C for 4 h. Pure Ag_2O using 0.02 mol $AgNO_3$ were also synthesized by the similar method in the absence of F-TiO_2. For the electrochemical impedance spectra (EIS) testing, the as-synthesized composites with 5 wt% cellulose binder were homogenously mixed in terpineol to form a slurry. Then, the resultant slurries were coated on the FTO using a screen-printing approach. Finally, these prepared electrodes were dried at 100 °C for 30 min.

2.3. Characterizations

The surface morphology, structure and composition of the samples were characterized by field-emission scanning electron microscopy (FESEM, Hitachi S-4800), high-resolution transmission electron microscopy (HRTEM, JEOL-2010), energy dispersive X-ray spectroscopy (EDS, JEM-2100, X-ray diffraction (XRD, Holland Panalytical PRO PW3040/60) with Cu Kα radiation (V = 30 kV, I = 25 mA), and Fourier transform infrared spectroscopy (FTIR, NICOLET NEXUS 670), respectively. The UV–vis diffuse absorption spectra of the samples were recorded using a Hitachi U-3900 UV–vis spectrophotometer equipped with an integrated sphere attachment. Photoluminescence (PL) spectra at room temperature were examined by fluorescence spectrophotometer (HORIBA Jobin Yvon fluoromax-4). X-ray photoelectron spectroscopy (XPS) measurement was performed on an Imaging Photoelectron Spectrometer (Axis Ultra, Kratos Analytical Ltd.) with a monochromatic Al Kα X-ray source. EIS measurements were carried out on an electrochemical workstation (AUTOLAB PGSTAT302N) under dark conditions using a three electrode configuration with the as-prepared films as working electrode, a Pt foil as counter electrode and a standard calomel electrode as reference electrode. The electrolyte was 10 mg l^{-1} MB aqueous solution. EIS were recorded in the frequency range of 0.1 Hz–1 MHz, and the applied bias voltage and ac amplitude were set at open-circuit voltage and 10 mV, respectively.

Table 1
Atomic ratios of Ag and F in T1, T2 and T3.

Samples	Ag (at.%)	F (at.%)
T1	7.23	2.33
T2	11.42	2.19
T3	14.59	2.12

2.4. Photocatalytic experiments

The photocatalytic performance of the as-prepared samples was evaluated by photocatalytic degradation of MB under visible light irradiation. The samples (120 mg) were dispersed in 80 ml MB solutions (10 mg/l). The mixed suspensions were first magnetically stirred in the dark for 30 min to reach the adsorption–desorption equilibrium. Under ambient conditions and stirring, the mixed suspensions were exposed to visible light irradiation ($\lambda > 400$ nm) produced by a 400 W metal halogen lamp with cut-off filter. At certain time intervals, 2 ml of the mixed suspensions were extracted and centrifuged to remove the photocatalyst. The filtrates were analyzed by recording UV–vis spectra of MB using a Hitachi U-3900 UV–vis spectrophotometer.

3. Results and discussion

The FESEM images of F-TiO_2 and Ag_2O are shown in Fig. 1(a) and (b). Both of the F-TiO_2 and Ag_2O display the particle nanostructure. The morphology of Ag_2O in AT composites (T2) is similar to that of pure Ag_2O, and the F-TiO_2 nanoparticles are well distributed in Ag_2O, as shown in Fig. 1(c). The morphologies of T1 and T3 (not shown here) are similar to that of T2. The existence of Ag_2O and F-TiO_2 in the composites is proved from elemental mapping image by EDS measurement, as shown in Fig. 1(d). Fig. 2 shows the element distribution, Ag, Ti and F elemental mapping images of T2. The distribution of Ag, Ti and F elements indicates that they are highly dispersed in the composites. Furthermore, the atomic ratios of Ag and F in T1, T2 and T3 were also characterized by the EDS, as shown in Table 1. It can be observed that the Ag_2O content in the composites increases with the increase of $AgNO_3$ in the precursor solution, while the F doping amount remains almost unchanged.

Fig. 3(a) and (b) shows the low-magnification and high-magnification HRTEM images of T2. It confirms the presence of F-TiO_2 nanoparticles with diameters in the range of 20–50 nm contacting with Ag_2O particles. The lattice fringes with an interplanar distance of 0.24 nm can be assigned to the (2 0 0) plane of Ag_2O (JCPDS 41-1104). Around the Ag_2O crystallite edge, fine crystallites are observed. The crystallites connected to the Ag_2O have lattice fringes of 0.35 nm, which is ascribed to the (1 0 1) plane of anatase F-TiO_2 (JCPDS 21-1272) [26].

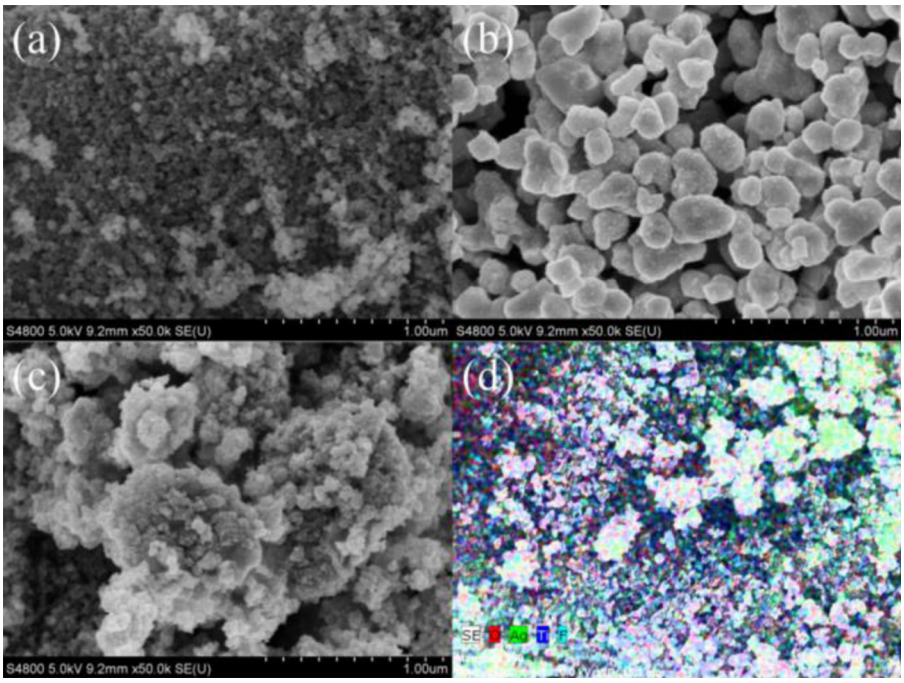

Fig. 1. FESEM images of (a) F-TiO_2, (b) Ag_2O and (c) T2; (d) EDS elemental mapping image of T2.

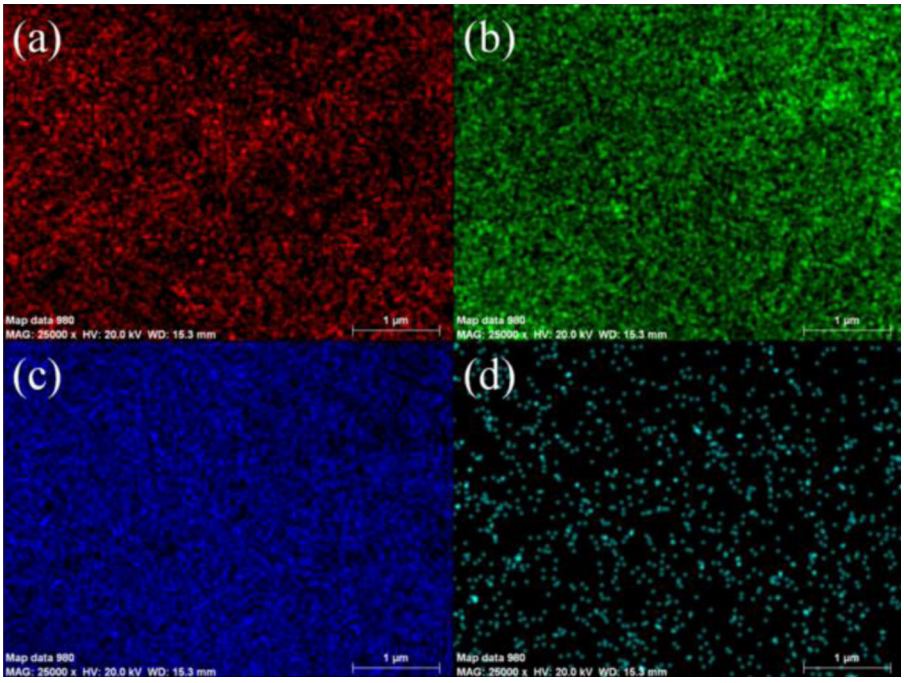

Fig. 2. (a) O, (b) Ag, (c) Ti and (d) F elemental mapping image by EDS measurement of T2.

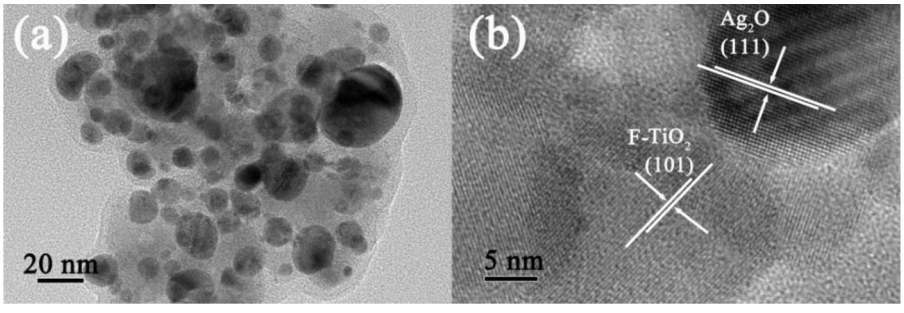

Fig. 3. (a) Low-magnification and (b) high-magnification HRTEM images of T2.

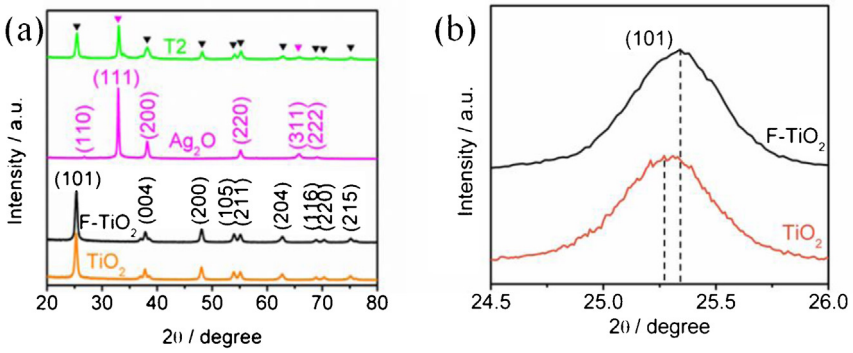

Fig. 4. XRD patterns of Ag_2O, TiO_2, F-TiO_2 and T2.

The XRD patterns of Ag_2O, TiO_2, F-TiO_2 and T2 are shown in Fig. 4. The peaks in the Ag_2O pattern at 26.6°, 32.8°, 38.3°, 54.9°, 65.4° and 68.7° are indexed to (1 1 0), (1 1 1), (2 0 0), (2 2 0), (3 1 1) and (2 2 2) planes of cubic Ag_2O (JCPDS 41-1104), respectively [42]. The main diffraction peaks of F-TiO_2 are similar to those of pure TiO_2, which can be indexed to the anatase TiO_2 (JCPDS 21-1272). Furthermore, as shown in Fig. 4(b), the F doping causes the shift of the TiO_2 peak to a larger angle. Compared with F-TiO_2, the new peaks corresponding to cubic phase of Ag_2O appear in XRD pattern of T2, which further confirms the existence of Ag_2O in the composite. No other impurity peaks for T2 are observed, indicating the high purity of the products.

Fig. 5 shows the FTIR spectra of F-TiO_2, Ag_2O, T1, T2 and T3. The broad absorption bands at 3425 cm^{-1} and 1661 cm^{-1} are assigned to the hydroxyl groups of absorbed H_2O molecules [42,43]. The absorption peak of Ag_2O around 500 cm^{-1} is related to Ag—O bond vibration [44]. The absorption band of AT composites at 650 cm^{-1} is similar to that of F-TiO_2, which is owing to the stretching modes of Ti—O [43]. Compared with the F-TiO_2, new absorption peak around 500 cm^{-1} appears in FTIR spectra of AT composites, which also proves the existence of Ag_2O in the composite.

The surface chemical composition of T2 was characterized by XPS measurements. Fig. 6(a) demonstrates the high-resolution XPS

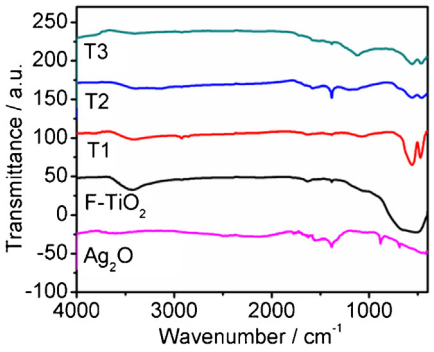

Fig. 5. FTIR spectra of F-TiO_2, Ag_2O, T1, T2 and T3.

spectrum of Ag 3d, displaying the spin-orbit split lines of Ag $3d_{3/2}$ and Ag $3d_{5/2}$ at 368.2 and 374.2 eV, respectively, which indicates that the Ag exists in one valence state (Ag^+) and further confirms the existence of Ag_2O in the composite [45,46]. Fig. 6(b) shows the high-resolution XPS spectrum of Ti 2p, displaying the spin–orbit split lines of Ti $2p_{3/2}$ and Ti $2p_{1/2}$ at 458.7 and 464.6 eV, respectively, which is in good agreement with that in TiO_2. As shown in Fig. 6(c),

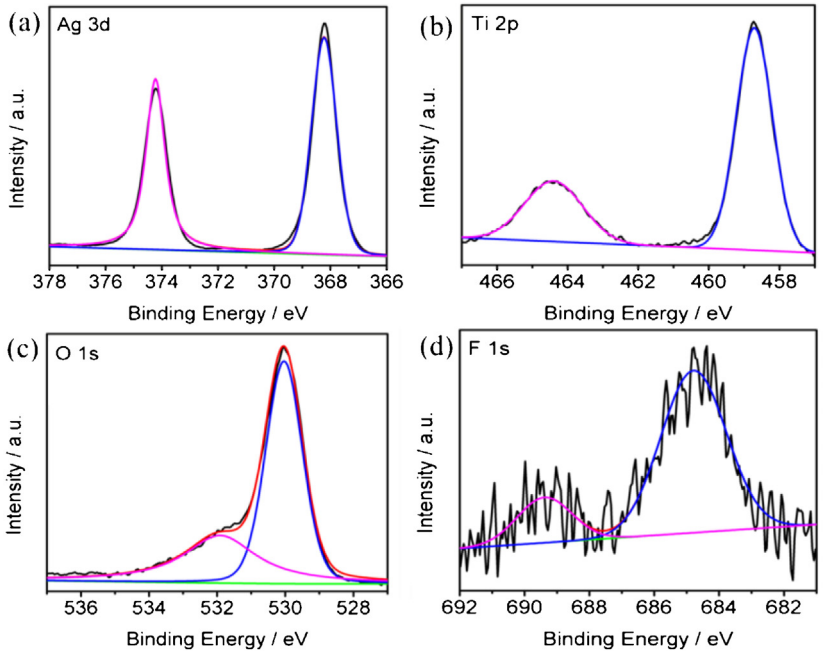

Fig. 6. XPS spectra of (a) Ag 3d, (b) Ti 2p, (c) O 1s, and (d) F 1s for T2.

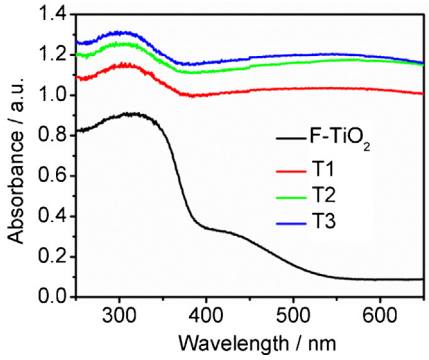

Fig. 7. UV–vis diffuse absorption spectra of F-TiO_2, T1, T2 and T3.

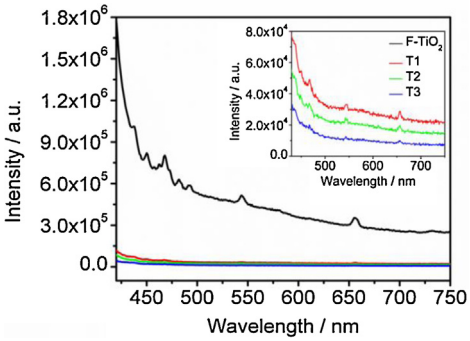

Fig. 9. PL spectra of F-TiO_2, T1, T2, and T3.

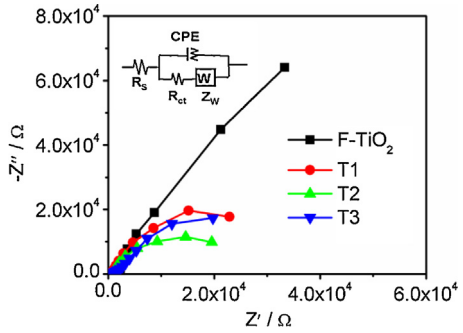

Fig. 8. Nyquist plots of F-TiO_2, T1, T2, and T3. Inset is the corresponding equivalent circuit model.

the O 1s spectrum of T2 is fitted to two peaks. The peak of O 1s at 530 eV corresponds to lattice oxygen of TiO_2, and a higher binding energy of 531.7 eV is assigned to mixed contributions from surface hydroxides. Fig. 6(d) gives the high-resolution XPS spectrum of F 1s. The F 1s peak can be deconvoluted into two peaks with Gaussian distributions, which indicates that two forms of F are present. The low binding energy of about 684.8 eV could be ascribed to the F anions physically adsorbed on the surface of TiO_2, while the high binding energy located at 689.3 eV could be ascribed to the F atoms substituting for the O atoms, forming the Ti—F bonds. The F content in the T2 is 2.58 at.%, which is almost consistent with the result of EDS measurement.

The UV–vis diffuse absorption spectra of F-TiO_2, T1, T2 and T3 are shown in Fig. 7. It is observed that the AT composites exhibit higher absorbance in the visible light region and the intensity increases with the increase of Ag_2O content, which is similar to those reported in the literatures [29,47]. Such an enhancement of light absorption is beneficial to the increase of photo-generated electrons and holes [43,48,49].

The charge transfer and recombination behaviors of the samples were studied by analyzing the EIS spectra under dark conditions. Fig. 8 shows the typical Nyquist plots of F-TiO_2, T1, T2 and T3. The semicircle in the EIS spectra is due to the contribution from the charge transfer resistance (R_{ct}) and constant phase element (CPE) at the photocatalyst/electrolyte interface [48,49]. The corresponding equivalent circuit is shown in the inset of Fig. 8. It is clearly observed that the R_{ct} decreases with the increase of Ag_2O content, which indicates that the introduction of Ag_2O in F-TiO_2 favors the electron transfer and suppresses the charge recombination in F-TiO_2 due to the stepwise energy level structure in the composites. However, when the Ag_2O content is further increased (T3), the R_{ct} increases, which is possibly because excessive Ag_2O can act as recombination centers instead of providing an electron pathway and promote the recombination of electron–hole pairs [29].

Fig. 9 shows PL spectra of F-TiO_2, T1, T2, and T3 with the excitation wavelength at 400 nm. It can be clearly observed that the introduction of Ag_2O markedly decreases the PL intensity, which further confirms that the recombination of photo-induced electrons and holes in F-TiO_2 can be effectively inhibited.

Photocatalytic degradation of MB by F-TiO_2, T1, T2 and T3 was performed under visible light irradiation. Fig. 10(a) shows the UV–vis absorption spectra of MB with the irradiation time under visible light irradiation using T2. It is observed that the UV–vis absorption peak of MB, related to its concentration in the solution, becomes weak with the increase in the irradiation time. Fig. 10(b) displays the time-dependent degradation rates of MB by F-TiO_2, Ag_2O, T1, T2, T3 and without catalyst under visible light irradiation. The normalized temporal concentration changes (C/C_0) of MB during the photocatalytic process are proportional to the normalized maximum absorbance (A/A_0), which can be derived from the change in the MB absorption profile at a given time interval. It is observed that the concentration of MB is hardly reduced under visible light irradiation in the absence of the photocatalyst, and the AT composites exhibit better photocatalytic activity than F-TiO_2 and Ag_2O. The photocatalytic activity of AT composites is dependent on the proportion of Ag_2O in the composites. The degradation rate of MB for F-TiO_2 and Ag_2O are 30% and 63% for 60 min, respectively. When Ag_2O is introduced into F-TiO_2, the degradation rate is increased to 81% for T1 and reaches a maximum value of 93% for T2 for 60 min. It is known that during photocatalysis, the light adsorption, and the charge transportation and separation are crucial factors [50–52]. The enhancement of the photocatalytic activity should be mainly ascribed to the increase in light absorption and the reduction in electron–hole pair recombination in F-TiO_2 with the introduction of Ag_2O due to the stepwise energy level in the composites, which have been confirmed by the UV–vis absorption, EIS and PL measurements. Furthermore, the self-sensitized degradation of the dyes should also play a critical role in the improvement of photocatalytic performance of AT composites under visible light irradiation. MB is excited under visible light irradiation to MB*, followed by photo-induced electrons transferring from MB* to Ag_2O or F-TiO_2, which react with adsorbed oxidants, usually O_2, to produce reactive oxygen radicals (O_2^-) [53]. This leads to the enhancement of photocatalytic performance. However, when the Ag_2O content is further increased, the degradation rate decreases to 87% for T3 at 60 min, which may be due to its increased recombination of photo-generated electron–hole pairs [29,47]. Furthermore, the repeatability of as-prepared samples was also investigated under visible light irradiation with three times of cycling uses, and the experimental error bars are shown in Fig. 10(b). It can be observed that the experimental error is small, showing that the experiment results are repeatable.

The values of rate constants (K_{app}), as shown in Fig. 11, can be obtained directly from the fitted straight-line plots of ln (C_0/C_t)

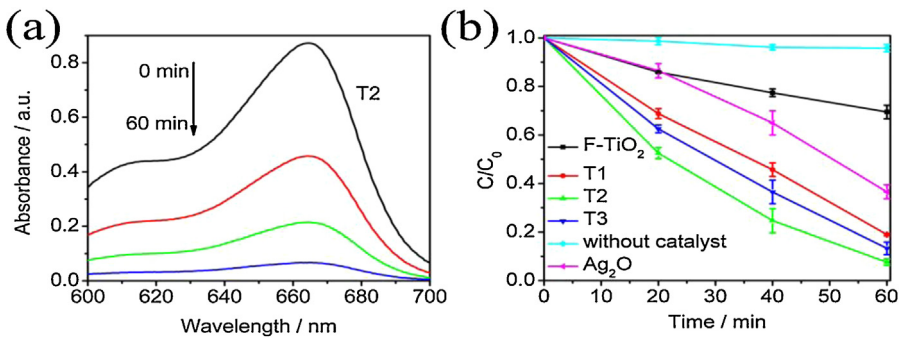

Fig. 10. (a) UV–vis absorbance of MB with the variation of visible light irradiation time using T2, (b) photocatalytic degradation of MB by F-TiO_2, Ag_2O, T1, T2, T3 and without catalyst under visible light irradiation.

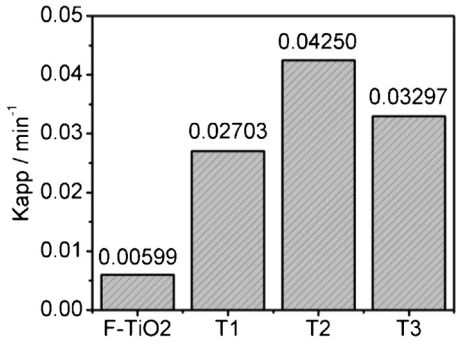

Fig. 11. Reaction constant K_{app} for MB degradation by F-TiO_2, T1, T2 and T3 using pseudo-first order kinetic equation.

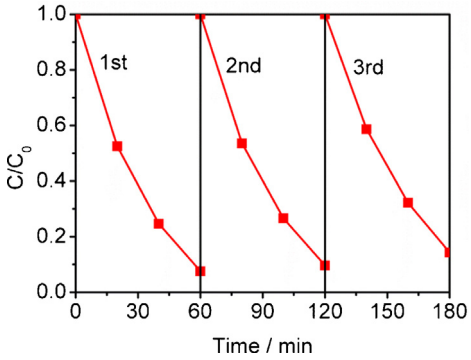

Fig. 12. Photo-stability of T2 by investigating its photocatalytic activity under visible light irradiation with three times of cycling uses.

vs. reaction time t and follow the order: T2 ($0.04250\,min^{-1}$) > T3 ($0.03297\,min^{-1}$) > T1 ($0.02703\,min^{-1}$) > F-TiO_2 ($0.00599\,min^{-1}$), where C_0 and C_t are the initial concentration and the concentration of MB at reaction time t (mg/l), respectively. The result confirms that T2 exhibits a best photocatalytic activity under visible light irradiation.

The stability of photocatalysts is very important for practical application. The photo-stability of AT composite (T2) was investigated under visible light irradiation with three times of cycling uses, as shown in Fig. 12. It is noteworthy that the recycled use of T2 for three times does not conspicuously affect its photocatalytic activity. Apparently, the composite is stable under the studied conditions. This self-stable mechanism of Ag_2O has been revealed by Wang et al. [54] and other previous works also demonstrated that the obtained Ag_2O/Ag exhibited a stable structure [34,35].

4. Conclusion

AT composites were successfully synthesized *via* an aqueous precipitation method and their photocatalytic activities under visible light irradiation were investigated. Results indicate that (1) AT composites exhibit an enhanced photocatalytic activity than F-TiO_2; (2) the photocatalytic activity of AT composites is dependent on the proportion of Ag_2O in the composites and the T2 achieves a highest MB degradation rate of 93% for 60 min; (3) the enhanced photocatalytic activity is mainly ascribed to the increase in light adsorption and the reduction in photoelectron–hole pair recombination with the introduction of Ag_2O.

Acknowledgements

Financial support from the National Natural Science Foundation of China (No. 21401180), Provincial Natural Science Foundation of Anhui (1508085ME104), and Scientific Research Foundation for the Anhui Provincial Returned Overseas Chinese Scholars (Electrospun low dimensional TiO_2 nano-structures and application in photovoltaic devices) is gratefully acknowledged.

References

[1] J.H. Yang, D. Wang, H.X. Han, C. Li, Acc. Chem. Res. 46 (2013) 1900–1909.
[2] W.G. Tu, Y. Zhou, Q. Liu, S.C. Yan, S.S. Bao, X.Y. Wang, M. Xiao, Z.G. Zou, Adv. Funct. Mater. 23 (2013) 1743–1749.
[3] Z.H. Ai, S.C. Lee, Appl. Surf. Sci. 280 (2013) 354–359.
[4] X. Li, J.G. Yu, J.X. Low, Y.P. Fang, J. Xiao, X.B. Chen, J. Mater. Chem. A 3 (2015) 2485–2534.
[5] Z.R. Tang, Y.H. Zhang, Y.J. Xu, RSC Adv. 1 (2011) 1772–1777.
[6] X.J. Bai, L. Wang, Y.J. Wang, W.Q. Yao, Y.F. Zhu, Appl. Catal. B: Environ. 152–153 (2014) 262–270.
[7] H. Tong, S.X. Ouyang, Y.P. Bi, N. Umezawa, M. Oshikiri, J.H. Ye, Adv. Mater. 24 (2012) 229–251.
[8] F.Y. Shen, W.X. Que, Y.C. He, Y. Yuan, X.T. Yin, G.F. Wang, ACS Appl. Mater. Interfaces 4 (2012) 4087–4092.
[9] H. Ming, Z. Ma, Y. Liu, K.M. Pan, H. Yu, F. Wang, Z.H. Kang, Dalton Trans. 41 (2012) 9526–9531.
[10] X.Y. Meng, G.H. Tian, Y.J. Chen, Y. Qu, J. Zhou, K. Pan, W. Zhou, G.L. Zhang, H.G. Fu, RSC Adv. 2 (2012) 2875–2881.
[11] X.Q. An, C.Y. Jimmy, RSC Adv. 1 (2011) 1426–1434.
[12] Q.J. Xiang, J.G. Yu, M. Jaroniec, Chem. Soc. Rev. 41 (2012) 782–796.
[13] X.J. Liu, L.K. Pan, T. Lv, Z. Sun, C.Q. Sun, RSC Adv. 2 (2012) 3823–3827.
[14] S. Zhan, F. Zhou, N.B. Huang, Y.F. Yin, M. Wang, Y.F. Yang, Y.J. Liu, J. Mol. Catal. A: Chem. 401 (2015) 41–47.
[15] N.A.S. Al-Areqi, A. Al-Alas, A.S.N. Al-Kamali, K.A.S. Ghaleb, K. Al-Mureish, J. Mol. Catal. A: Chem. 381 (2014) 1–8.
[16] K. Kang, M. Jang, M.C. Cui, P.P. Qiu, B. Park, S.A. Snyder, J. Khim, J. Mol. Catal. A: Chem. 390 (2014) 178–186.
[17] J.C. Sun, Y.B. Zhang, J. Cheng, H. Fan, J.Y. Zhu, X. Wang, S.Y. Ai, J. Mol. Catal. A: Chem. 382 (2014) 146–153.
[18] A. Hamrouni, N. Moussa, F. Parrino, A. Di Paola, A. Houas, L. Palmisano, J. Mol. Catal. A: Chem. 390 (2014) 133–141.
[19] Y.P. Yuan, L.W. Ruan, J. Barber, S.C.J. Loo, C. Xue, Energy Environ. Sci. 7 (2014) 3934–3951.
[20] J.G. Yu, Q. Li, S.W. Liu, M. Jaroniec, Chem. Eur. J. 19 (2013) 2433–2441.
[21] H.H. Li, S. Yin, Y.H. Wang, T. Sato, Environ. Sci. Technol. 46 (2012) 7741–7745.

[22] G.D. Yang, T.C. Xiao, J. Sloan, G.Q. Li, Z.F. Yan, Chem. Eur. J. 17 (2011) 1096–1100.
[23] J.K. Zhou, L. Lv, J.Q. Yu, H.L. Li, P.Z. Guo, H. Sun, X.S. Zhao, J. Phys. Chem. C 112 (2008) 5316–5321.
[24] Z.F. Zhu, J.Q. Zhou, Z.L. He, J.Q. Li, H. Liu, Mater. Res. Innov. 15 (2011) 78–82.
[25] D. Li, H. Haneda, N.K. Labhsetwar, S. Hishita, N. Ohashi, Chem. Phys. Lett. 401 (2005) 579–584.
[26] W. Yu, X.J. Liu, L.K. Pan, J.L. Li, J.Y. Liu, J. Zhang, P. Li, C. Chen, Z. Sun, Appl. Surf. Sci. 319 (2014) 107–112.
[27] D.G. Huang, S.J. Liao, S.Q. Quan, L. Liu, Z.J. He, J.B. Wan, W.B. Zhou, J. Mater. Sci. 42 (2007) 8193–8202.
[28] M.V. Dozzi, S. Livraghi, E. Giamello, E. Selli, Photochem. Photobiol. Sci. 10 (2011) 343–349.
[29] J.Y. Liu, X.J. Liu, J.L. Li, L.K. Pan, Z. Sun, RSC Adv. 4 (2014) 38594–38598.
[30] C. Shifu, Y. Yunguang, L. Wei, J. Hazard. Mater. 186 (2011) 1560–1567.
[31] Z. Jin Feng, Y. Yun Guang, L. Wei, Int. J. Photoenergy 2012 (2012).
[32] W.F. Yao, B. Zhang, C.P. Huang, C. Ma, X.L. Song, Q.J. Xu, J. Mater. Chem. 22 (2012) 4050–4055.
[33] X.F. Wang, S.F. Li, H.G. Yu, J.G. Yu, S.W. Liu, Chem. Eur. J. 17 (2011) 7777–7780.
[34] H.G. Yu, R. Liu, X.F. Wang, P. Wang, J.G. Yu, Appl. Catal. B: Environ. 111–112 (2012) 326–333.
[35] L. Shi, L. Liang, J. Ma, F.X. Wang, J.M. Sun, Catal. Sci. Technol. 4 (2014) 758–765.
[36] M. Wu, J.M. Yan, M. Zhao, Q. Jiang, ChemPlusChem 77 (2012) 931–935.
[37] C. Yu, G. Li, S. Kumar, K. Yang, R. Jin, Adv. Mater. 26 (2014) 892–898.
[38] L. Zhu, B. Wei, L.L. Xu, Z. Lu, H.L. Zhang, H. Gao, J.X. Che, CrystEngComm 14 (2012) 5705–5709.
[39] Y. Xu, M.A. Schoonen, Am. Mineral. 85 (2000) 543–556.
[40] R. Asahi, T. Morikawa, T. Ohwaki, K. Aoki, Y. Taga, Science 293 (2001) 269–271.
[41] S.S. Ma, J.J. Xue, Y.M. Zhou, Z.W. Zhang, J. Mater. Chem. A 2 (2014) 7272–7280.
[42] M. Xu, L. Han, S. Dong, ACS Appl. Mater. Interfaces 5 (2013) 12533–12540.
[43] X.J. Liu, L.K. Pan, T. Lv, G. Zhu, T. Lu, Z. Sun, C.Q. Sun, RSC Adv. 1 (2011) 1245–1249.
[44] N.L. Yong, A. Ahmad, A.W. Mohammad, Int. J. Sci. Eng. Res. 4 (2013) 155–158.
[45] Y. Ida, S. Watase, T. Shinagawa, M. Watanabe, M. Chigane, M. Inaba, A. Tasaka, M. Izaki, Chem. Mater. 20 (2008) 1254–1256.
[46] J. Hammond, S. Gaarenstroom, N. Winograd, Anal. Chem. 47 (1975) 2193–2199.
[47] O. Kerkez, İ. Boz, Chem. Eng. Commun. 202 (2014) 534–541.
[48] X.J. Liu, X.J. Wang, H.L. Li, J.L. Li, L.K. Pan, J. Zhang, G.Q. Min, Z. Sun, C.Q. Sun, Dalton Trans. 44 (2015) 97–103.
[49] X.J. Liu, X.J. Wang, H.L. Li, L.K. Pan, T. Lv, Z. Sun, C.Q. Sun, J. Mater. Chem. 22 (2012) 16293–16298.
[50] H. Zhang, X.J. Lv, Y.M. Li, Y. Wang, J.H. Li, ACS Nano 4 (2009) 380–386.
[51] X.J. Liu, L.K. Pan, T. Lv, Z. Sun, C.Q. Sun, J. Colloid Interface Sci. 408 (2013) 145–150.
[52] X.J. Liu, L.K. Pan, T. Lv, G. Zhu, Z. Sun, C.Q. Sun, Chem. Commun. 47 (2011) 11984–11986.
[53] Z.G. Xiong, L.L. Zhang, J.Z. Ma, X.S. Zhao, Chem. Commun. 46 (2010) 6099–6101.
[54] X. Wang, S. Li, H. Yu, J. Yu, S. Liu, Chem. Eur. J. 17 (2011) 7777–7780.